This article has been accepted for publication in a future issue of this journal, but has not been fully edited. Content may change prior to final publication. Citation information: DOI10.1109/lwc.2023.3243031, IEEE Wireless Communications Letters

Joint Optimization for Cooperative Computing Framework in Double-IRS-Aided MEC Systems

Yi Zhou, Cunhua Pan, Phee Lep Yeoh, Kezhi Wang, Zheng Ma, Branka Vucetic and Yonghui Li

***Abstract*—This letter investigates a cooperative task computing framework, where the source node partially offloads its computational task to multiple user equipments (UEs) aided by double intelligent reflecting surfaces (IRSs). With the aim of maximizing the total amount of computing task subject to latency and power constraints, we highlight an interesting tradeoff between the transmit power and the computing power at the source node and optimize the computing frequency resources as well as phase shift matrices for double IRSs. Numerical results verify the power allocation tradeoff and demonstrate the superiority of our double-IRS-aided solution in terms of maximizing the total amount of computing task over other benchmark strategies.**

***Index Terms*—Double-IRS, cooperative computing, MEC.**

I. Introduction

Mobile edge computing (MEC) has been envisioned as a key technology in fifth-generation (5G) and sixth-generation (6G) communications [1], [2]. In [3], a heterogeneous multi-layer MEC network was proposed to reduce the system latency and increase the processing rate by efficiently utilizing the computing and transmission resources. To further explore the possibilities on reducing latency, cooperative computing was adopted in [4] to support latency-sensitive applications by embedding computing resources at each user equipment (UE), where a cost minimization problem was studied by considering the power consumption and penalty for unaccomplished tasks. However, when the wireless propagation channels between UEs are blocked by obstacles or suffer from high attenuation, the performance of MEC-enabled cooperative computing systems cannot be guaranteed.

To tackle this issue, intelligent reflecting surface (IRS), which is capable of reconfiguring the transmission environment of the wireless propagation channels, has been proposed as a novel enabler for providing additional transmission links and expanding the communication coverage [5], [6]. An IRS is a metasurface which consists of an array of reflecting elements, each of which can be configured to reflect the transmission signal intelligently by adjusting its amplitude and phase shift [7], [8]. In [9], a weighted latency minimization solution was proposed in an IRS-aided MEC system by jointly optimizing the offloading ratio, computing resources and IRS phase shift. In [10], a partial offloading scheme was adopted in an IRS-assisted device-to-device (D2D) cooperative computing system to minimize the total computing delay.

However, most of the IRS-related works have focused on the deployment of one single IRS or multiple non-cooperative IRSs with single-reflection channel, where the performance improvement benefiting from the mutual impact between IRSs has not been fully investigated. Deploying double IRSs with joint consideration of double-reflection link, single-reflection link and direct link provides new possibilities on improving the transmission rate. Recently, the authors in [11] proposed a double-IRS-aided communication framework, where the double-reflection link between IRSs was considered to further improve the communication performance. Notably, no prior works have discussed the advantages of double-IRS with double-reflection link on improving the computing performance in an MEC-enabled cooperative computing system, thus motivating this work.

In this letter, we propose a novel double-IRS-aided cooperative computing framework where the source node partially offloads its computational task to multiple UEs via the direct link, single-reflection link and double-reflection link. We highlight the contributions of our work from the following perspectives. First, we discuss the tradeoff between the computing power and the transmit power at the source node. Based on this, we investigate the computing frequency resource allocation among all UEs under a total power budget in terms of achieving the maximum amount of computing task. Then, the potential advantages of double-IRS in assisting the cooperative computing are investigated by jointly optimizing the phase shift matrices of double IRSs. To do so, we propose an efficient optimization solution using the alternating optimization (AO), Karush-Kuhn-Tucker (KKT) conditions and semi-definite relaxation (SDR) methods. Finally, numerical results are provided to verify the power allocation tradeoff and demonstrate the superiority of our double-IRS-aided cooperative computing algorithm over other benchmark strategies.

Notations: $\mathrm{diag}(\boldsymbol{z})$ and $\boldsymbol{z}^{\boldsymbol{H}}$ represent the diagonalization and Hermitian transpose of a complex-valued vector $\boldsymbol{z}$, respectively. $\boldsymbol{Z}_{i,j}$, $\mathrm{Tr}(\boldsymbol{Z})$ and $\mathrm{rank}(\boldsymbol{Z})$ represent the the $(i,j)th$ element, trace and rank of matrix $\boldsymbol{Z}$, respectively.

II. System Model

As shown in Fig. 1, we consider a double-IRS aided cooperative computing system where one source node partially

The work of Y. Zhou was supported by Natural Science Foundation of Sichuan Province under Grant 2022NSFSC0887 and the Fundamental Research Funds for the Central Universities under Grant 2682021ZTPY117 and 2682022CX020. The work of C. Pan was supported by the National Natural Science Foundation of China under Grant 62201137. The work of Z. Ma was supported by the National Natural Science Foundation of China under Grant 62271419. The work of B. Vucetic was supported in part by the Australian Research Council Laureate Fellowship grant number FL160100032. The work of Y. Li was supported by ARC under Grant DP190101988 and DP210103410.

Y. Zhou and Z. Ma are with the Key Lab of Information Coding, and Transmission, Southwest Jiaotong University, Chengdu 610031, China. (e-mail:yizhou@swjtu.edu.cn;zma@home.swjtu.edu.cn).

C. Pan is with the National Mobile Communications Research Laboratory, Southeast University, China. (e-mail:cpan@seu.edu.cn).

P. L. Yeoh, B. Vucetic, and Y. Li are with the School of Electrical and Information Engineering, University of Sydney, NSW 2006, Australia (e-mail: {phee.yeoh, branka.vucetic, yonghui.li}@sydney.edu.au).

K. Wang is with Department of Computer Science, Brunel University London, Uxbridge, Middlesex, UB8 3PH (email: kezhi.wang@brunel.ac.uk)

This article has been accepted for publication in a future issue of this journal, but has not been fully edited. Content may change prior to final publication. Citation information: DOI10.1109/lwc.2023.3243031, IEEE Wireless Communications Letters

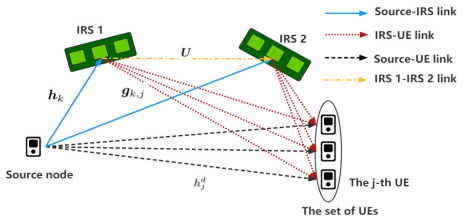

Fig. 1. A double-IRS-aided cooperative computing system.

offloads its computational task to J UEs aided by double IRSs via frequency division multiple access (FDMA). We consider that each IRS employs a uniform linear array (ULA) with N reflecting elements and define the set of UEs and reflecting elements on each IRS as $\mathcal{J}$ and $\mathcal{N}$, respectively. The source node and all UEs are equipped with a single antenna. Define the phase shift of the n-th element in the k-th $\forall k \in \{1,2\}$ IRS as $\omega_{k,n} \in [0, 2\pi]$. Thus, the diagonal phase shift matrix for the k-th IRS is $\boldsymbol{\Phi}_k = \text{diag}\{\boldsymbol{\theta}_k\}$ with $\boldsymbol{\theta}_k = [e^{j\omega_{k,1}}, e^{j\omega_{k,2}}, \cdots, e^{j\omega_{k,n}}], \forall n \in \mathcal{N}, \forall k \in \{1,2\}$.

A. Communication Model

All channels are modeled as Rician fading channels. Define the equivalent channels from the source node to the k-th IRS, from the source node to the j-th UE, from the k-th IRS to the j-th UE and from IRS 1 to IRS 2 as $\boldsymbol{h}_k \in \mathbb{C}^{N\times 1}$, $h_j^d \in \mathbb{C}^{1\times 1}$, $\boldsymbol{g}_{k,j} \in \mathbb{C}^{N\times 1}$ and $\boldsymbol{U} \in \mathbb{C}^{N\times N}$, respectively. As such, the achievable rate at the j-th UE is given by [11]

$$R_j = \log_2\left(1 + \frac{p|\sum_{k=1}^{2} \boldsymbol{g}_{k,j}^{\boldsymbol{H}} \boldsymbol{\Phi}_k \boldsymbol{h}_k + \boldsymbol{g}_{2,j}^{\boldsymbol{H}} \boldsymbol{S} \boldsymbol{h}_1 + h_j^d|^2}{\sigma^2}\right), \forall j, \tag{1}$$

where p is the transmit power at the source node toward each UE, σ^2 is the noise power, $\boldsymbol{g}_{2,j}^{\boldsymbol{H}} \boldsymbol{S} \boldsymbol{h}_1$ represents the channel gain of the double-reflection link from the source node to the UEs via IRS 1 and IRS 2 with $\boldsymbol{S} \in \mathbb{C}^{N\times N} = \boldsymbol{\Phi}_2 \boldsymbol{U} \boldsymbol{\Phi}_1$. [1]

Next, we define $\boldsymbol{v} = [\theta_{1,1}, \cdots, \theta_{1,n}]^{\boldsymbol{T}}$ and $\boldsymbol{r} = [\theta_{2,1}, \cdots, \theta_{2,n}]^{\boldsymbol{T}}$ with $\theta_{1,n} = e^{jw_{1,n}}, \theta_{2,n} = e^{jw_{2,n}}, \forall n \in \mathcal{N}$, respectively. We further define $\boldsymbol{\Psi}_{1,j} = \boldsymbol{g}_{1,j}^{\boldsymbol{H}} \text{diag}(\boldsymbol{h}_1)$ and $\boldsymbol{\Psi}_{2,j} = \boldsymbol{g}_{2,j}^{\boldsymbol{H}} \text{diag}(\boldsymbol{h}_2)$, which result in $\boldsymbol{g}_{1,j}^{\boldsymbol{H}} \boldsymbol{\Phi}_1 \boldsymbol{h}_1 = \boldsymbol{\Psi}_{1,j} \boldsymbol{v}$, $\boldsymbol{g}_{2,j}^{\boldsymbol{H}} \boldsymbol{\Phi}_2 \boldsymbol{h}_2 = \boldsymbol{\Psi}_{2,j} \boldsymbol{r}$. To proceed, we let $\bar{\boldsymbol{U}} = \boldsymbol{U}\text{diag}(\boldsymbol{h}_1) = [\boldsymbol{u}_{1,1}, \cdots, \boldsymbol{u}_{1,N}]$, thus, we have

$$\begin{aligned} \boldsymbol{g}_{2,j}^{\boldsymbol{H}} \boldsymbol{S} \boldsymbol{h}_1 &= \boldsymbol{g}_{2,j}^{\boldsymbol{H}} \boldsymbol{\Phi}_2 \boldsymbol{U} \boldsymbol{\Phi}_1 \boldsymbol{h}_1 = \boldsymbol{g}_{2,j}^{\boldsymbol{H}} \boldsymbol{\Phi}_2 \bar{\boldsymbol{U}} \boldsymbol{v} \\ &= \boldsymbol{g}_{2,j}^{\boldsymbol{H}} [\boldsymbol{\Phi}_2 \boldsymbol{u}_{1,1}, \cdots, \boldsymbol{\Phi}_2 \boldsymbol{u}_{1,N}] \boldsymbol{v} \\ &= \boldsymbol{g}_{2,j}^{\boldsymbol{H}} [\text{diag}(\boldsymbol{u}_{1,1}) \boldsymbol{r}, \cdots, \text{diag}(\boldsymbol{u}_{1,N}) \boldsymbol{r}] \boldsymbol{v} \\ &= \sum_{n=1}^{N} \underbrace{\boldsymbol{g}_{2,j}^{\boldsymbol{H}} \text{diag}(\boldsymbol{u}_{1,n})}_{\boldsymbol{S}_{n,j}} \boldsymbol{r} v_n. \end{aligned} \tag{2}$$

Thus, the achievable rate at the j-th UE can be rewritten as

$$R_j = \log_2\left(1 + \frac{p|\boldsymbol{\Psi}_{1,j} \boldsymbol{v} + \boldsymbol{\Psi}_{2,j} \boldsymbol{r} + \sum_{n=1}^{N} \boldsymbol{S}_{n,j} \boldsymbol{r} v_n + h_j^d|^2}{\sigma^2}\right), \forall j. \tag{3}$$

[1]We note that there exists another longer double-reflection link given by the source-IRS 2-IRS 1-UEs transmission path in Fig. 1 which is omitted in Eq. (1) due to the associated higher path loss [11].

For reflection links, it can be seen from (3) that the cascaded channel state information (CSI) of $\boldsymbol{S}_{n,j}$, $\boldsymbol{\Psi}_{1,j}$ and $\boldsymbol{\Psi}_{2,j}$ is sufficient to design the double-IRS-aided cooperative computing framework, which can be accurately estimated with relatively low overhead by adopting the proposed method in [12].

B. Computing Model

We consider a partial offloading scheme where the source node computes D_0 bits of the computational task locally and offloads D_j bits of the task to the j-th UE via double IRSs.

1) Latency Constraint: The latency for local computing is $t_0 = \frac{D_0 F}{f_0}$, where f_0 is the local computing frequency and F is the number of central processing unit (CPU) cycles required for processing one bit of the data.

When source node offloads its task to the j-th UE via double IRSs, the overall latency for offloading consists of transmission and computing latencies, i.e., $t_j = \frac{D_j F}{f_j} + \frac{D_j}{BR_j}$, where f_j is the computing frequency at the j-th UE, R_j is the achievable rate at the j-th UE as shown in (1) and B is the bandwidth allocated to each UE. Due to the small size of the computation results, the latency for returning the computation results is negligible [10].

Since the local computing and task offloading are processed simultaneously, thus, the maximum number of bits under a given latency T is given by

$$D_{tot} = \frac{T f_0}{F} + \sum_{j\in\mathcal{J}} \frac{T}{\frac{F}{f_j} + \frac{1}{BR_j}}. \tag{4}$$

2) Power Constraint: Due to the limited battery equipped on the source node, the total power consumed for computing and transmitting should be bounded by a maximum budget p_0^{max}, which is given by

$$\kappa {f_0}^3 + Jp \le p_0^{max}, \tag{5}$$

where κ is a constant, the value of which depends on the chip architecture.

For the set of UEs, we consider that the overall power consumption should be bounded by a budget p_{tot}, which is given by

$$\sum_{j\in\mathcal{J}} \kappa {f_j}^3 \le p_{tot}. \tag{6}$$

III. Problem Formulation and Proposed Solution

In this letter, we aim to maximize the total amount of computing task D_{tot} subject to latency and power constraints. We jointly optimize the source node's transmit power p, computing frequency allocation $\{f_0, f_j, \forall j \in \mathcal{J}\}$ as well as the phase shift matrices for double IRSs $\boldsymbol{\Phi}_k, \forall k \in \{1,2\}$. Thus, the optimization problem can be formulated as

$$\max_{p, f_0, f_j, \boldsymbol{\Phi}_2, \boldsymbol{\Phi}_1} \frac{T f_0}{F} + \sum_{j\in\mathcal{J}} \frac{T}{\frac{F}{f_j} + \frac{1}{B\log_2(1+pC_j)}} \tag{7a}$$

$$\text{s.t.} \quad \omega_{k,n} \in [0, 2\pi], \forall k \in \{1,2\}, \forall n \in \mathcal{N} \tag{7b}$$

$$\kappa {f_0}^3 + Jp \le p_0^{max} \tag{7c}$$

$$\sum_{j\in\mathcal{J}} \kappa {f_j}^3 \le p_{tot}, \tag{7d}$$

$$p > 0, f_0 \ge 0, f_j > 0, \forall j \in \mathcal{J}, \tag{7e}$$

This article has been accepted for publication in a future issue of this journal, but has not been fully edited. Content may change prior to final publication. Citation information: DOI10.1109/lwc.2023.3243031, IEEE Wireless Communications Letters

where $C_j = \frac{|\sum_{k=1}^{2} \boldsymbol{g}_{k,j}^{\boldsymbol{H}} \boldsymbol{\Phi}_k \boldsymbol{h}_k + \boldsymbol{g}_{2,j}^{\boldsymbol{H}} \boldsymbol{S} \boldsymbol{h}_1 + h_j^d|^2}{\sigma^2}$. Due to the coupling effects among all variables and the non-convexity of the objective function with respect to $\boldsymbol{\Phi}_1$ and $\boldsymbol{\Phi}_2$, Problem (7) is non-convex and difficult to solve. To tackle these issues, we apply the AO method and decouple Problem (7) into three subproblems to solve them in an iterative manner.

A. Solve Transmit Power and Computing Frequency at the Source Node

In this subsection, we solve $\{p, f_0\}$ with given $\{f_j, \boldsymbol{\Phi}_2, \boldsymbol{\Phi}_1\}$. Interestingly, we observe that increasing both the local computing frequency f_0 and the transmit power p results in an increase of D_{tot} according to (1) and (7a). Thus, the maximum D_{tot} can be achieved when (7c) holds with equality. By substituting f_0 with $\sqrt[3]{\frac{p_0^{max} - Jp}{\kappa}}$, the transmit power subproblem can be reformulated as

$$\max_{p_j} \frac{T\sqrt[3]{\frac{p_0^{max}-Jp}{\kappa}}}{F} + \sum_{j\in\mathcal{J}} \frac{T}{A_j + \frac{1}{B\log_2\left(1+pC_j\right)}} \tag{8a}$$

$$\text{s.t.} \quad 0 < Jp \le p_0^{max}, \tag{8b}$$

where $A_j = \frac{F}{f_j}$. To solve Problem (8) optimally, we analyze its convexity in the following lemma.

Lemma 1. *Problem* (8) *is a convex optimization problem.*

Proof. To show the convexity, we denote $g(p) = \sqrt[3]{\frac{p_0^{max}-Jp}{\kappa}}$ and $f(p) = \frac{T}{A_j + \frac{1}{B\log_2(1+pC_j)}}$. With $0 < Jp \le p_0^{max}$, we derive the second-order derivatives of $g(p)$ and $f(p)$ respectively as follows

$$\frac{\partial^2 g}{\partial p^2} = -\frac{2J^2}{9\kappa^2}\left(\frac{p_0^{max}-Jp}{\kappa}\right)^{-\frac{5}{3}} \le 0 \tag{9a}$$

$$\frac{\partial^2 f}{\partial p^2} = -\frac{TC_j^2 B(2A_jB/\ln 2 + A_jB\log_2(1+pC_j)+1)}{\ln 2(A_jB\log_2(1+pC_j)+1)^3(1+pC_j)^2} < 0. \tag{9b}$$

According to (9a) and (9b), we can see that both the first and the second terms in (8a) are concave with respect to p. With the aim of maximizing (8a), we show that Problem (8) is a convex optimization problem. □

With Lemma 1, it can be found that the optimal transmit power $p^* \in (0, p_0^{max}/J]$ is the solution when the first-order derivative of (8a) equals to 0, which satisfies

$$\sum_{j\in\mathcal{J}} \frac{TBC_j/(1+p^*C_j)}{\ln 2(A_jB\log_2(1+p^*C_j)+1)^2} - \frac{TJ\left(\frac{p_0^{max}-Jp^*}{\kappa}\right)^{-\frac{2}{3}}}{3F\kappa} = 0. \tag{10}$$

To solve (10), we adopt the bisection search method with a complexity of $\mathcal{O}(\log_2(1/\epsilon))$, where ϵ is the termination parameter. With the optimized p^*, the optimal local computing frequency f_0 is given by

$$f_0^* = \sqrt[3]{(p_0^{max} - Jp^*)/\kappa}. \tag{11}$$

B. Solve Computing Frequency Allocation for UEs

According to Problem (7), we observe that D_{tot} is positively related to f_j. Thus, with the aim of maximizing D_{tot}, (7d) should hold with equality. Given $\{p, f_0, \boldsymbol{\Phi}_2, \boldsymbol{\Phi}_1\}$, by removing the constant term and performing further mathematical manipulations, we formulate the computing frequency allocation subproblem for UEs as follows

$$\min_{f_j} \; -\sum_{j\in\mathcal{J}} \frac{T}{\frac{F}{f_j} + \frac{1}{BR_j}} \tag{12a}$$

$$\text{s.t.} \quad \sum_{j\in\mathcal{J}} \kappa {f_j}^3 = p_{tot}, f_j > 0. \tag{12b}$$

Since the second-order derivative of the objective function (12a) satisfies $\frac{2TF/B/R_j}{(F+f_j/B/R_j)^3} \ge 0$, we can see that Problem (12) is convex. Then, we apply the KKT conditions and derive the corresponding Lagrangian function as

$$\mathcal{L}(f_j, \mu) = -\sum_{j\in\mathcal{J}} \frac{T}{\frac{F}{f_j} + \frac{1}{BR_j}} + \mu\left(\sum_{j\in\mathcal{J}} \kappa {f_j}^3 - p_{tot}\right), \tag{13}$$

where μ is the non-negative Lagrange multiplier and the following KKT conditions should be satisfied

$$\frac{\partial \mathcal{L}}{\partial f_j} = -\frac{TF}{\left(F + \frac{f_j^*}{BR_j}\right)^2} + 3\mu^*\kappa(f_j^*)^2 = 0, \forall j \in \mathcal{J} \tag{14a}$$

$$\mu^*\left(\sum_{j\in\mathcal{J}} \kappa(f_j^*)^3 - p_{tot}\right) = 0 \quad \text{and} \quad f_j^* > 0, \forall j \in \mathcal{J}. \tag{14b}$$

Based on (14a), we derive the optimal computing frequencies for UEs as

$$f_j^* = \sqrt{BR_j\sqrt{\frac{TF}{3\kappa\mu^*}} + \left(\frac{FBR_j}{2}\right)^2} - \frac{FBR_j}{2}, \forall j \in \mathcal{J}. \tag{15}$$

Based on (12b), the optimal μ^* satisfies

$$\sum_{j\in\mathcal{J}} \kappa\left(\sqrt{BR_j\sqrt{\frac{TF}{3\kappa\mu^*}} + \left(\frac{FBR_j}{2}\right)^2} - \frac{FBR_j}{2}\right)^3 = p_{tot}, \tag{16}$$

and can be found by adopting the bisection search method with a complexity of $\mathcal{O}(\log_2(1/\epsilon))$.

C. Solve Phase Shift Matrices for Double IRSs

In this subsection, we solve the phase shift matrix for IRS 2 and IRS 1 alternately with fixed $\{p, f_0, f_j\}$. By introducing an auxiliary set $\boldsymbol{s} \triangleq \{s_j, \forall j \in \mathcal{J}\}$ representing the lower bound of R_j and removing the constant term, with given $\boldsymbol{\Phi}_1$, the phase shift matrix for IRS 2 can be derived by solving

$$\max_{\boldsymbol{\Phi}_2, \boldsymbol{s}} \sum_{j\in\mathcal{J}} \frac{T}{\frac{F}{f_j} + \frac{1}{Bs_j}} \tag{17a}$$

$$\text{s.t.} \quad |\boldsymbol{R}_j^{\boldsymbol{H}}\boldsymbol{r} + \eta_j|^2 \ge \frac{\sigma^2(2^{s_j}-1)}{p}, \forall j \in \mathcal{J} \tag{17b}$$

$$|r_n|^2 = 1, \forall n \in \mathcal{N}, \tag{17c}$$

where $\boldsymbol{R}_j^{\boldsymbol{H}} = \sum_{n=1}^{N} \boldsymbol{S}_{n,j} v_n + \boldsymbol{\Psi}_{2,j}, \eta_j = \boldsymbol{\Psi}_{1,j}\boldsymbol{v} + h_j^d$. We note that $|\boldsymbol{R}_j^{\boldsymbol{H}}\boldsymbol{r} + \eta_j|^2 = \boldsymbol{R}_j^{\boldsymbol{H}}\boldsymbol{r}\boldsymbol{r}^{\boldsymbol{H}}\boldsymbol{R}_j + \boldsymbol{R}_j^{\boldsymbol{H}}\boldsymbol{r}\eta_j^{\boldsymbol{H}} + \eta_j\boldsymbol{r}^{\boldsymbol{H}}\boldsymbol{R}_j + |\eta_j|^2$. In the following, we transform $|\boldsymbol{R}_j^{\boldsymbol{H}}\boldsymbol{r} + \eta_j|^2$ as

$$|\boldsymbol{R}_j^{\boldsymbol{H}}\boldsymbol{r} + \eta_j|^2 = \bar{\boldsymbol{r}}^{\boldsymbol{H}}\boldsymbol{Z}_j\bar{\boldsymbol{r}} + |\eta_j|^2, \tag{18}$$

where

$$\boldsymbol{Z}_j = \begin{bmatrix} \boldsymbol{R}_j\boldsymbol{R}_j^{\boldsymbol{H}} & \eta_j\boldsymbol{R}_j \\ \eta_j^{\boldsymbol{H}}\boldsymbol{R}_j^{\boldsymbol{H}} & 0 \end{bmatrix}, \bar{\boldsymbol{r}} = \begin{bmatrix} \boldsymbol{r} \\ 1 \end{bmatrix}. \tag{19}$$

This article has been accepted for publication in a future issue of this journal, but has not been fully edited. Content may change prior to final publication. Citation information: DOI10.1109/lwc.2023.3243031, IEEE Wireless Communications Letters

We further define $\boldsymbol{V}_2 = \bar{\boldsymbol{r}}\bar{\boldsymbol{r}}^{\boldsymbol{H}}$, where the constraint of $\boldsymbol{V}_2 \succeq 0$ and $\text{rank}(\boldsymbol{V}_2) = 1$ need to be satisfied. Since $\bar{\boldsymbol{r}}^{\boldsymbol{H}}\boldsymbol{Z}_j\bar{\boldsymbol{r}} = \text{Tr}(\boldsymbol{Z}_j\bar{\boldsymbol{r}}\bar{\boldsymbol{r}}^{\boldsymbol{H}})$, we have $\bar{\boldsymbol{r}}^{\boldsymbol{H}}\boldsymbol{Z}_j\bar{\boldsymbol{r}} = \text{Tr}(\boldsymbol{Z}_j\boldsymbol{V}_2)$. By relaxing the rank-one constraint, the phase shift matrix for IRS 2 can be derived by

$$\max_{\boldsymbol{V}_2,\boldsymbol{s}} \sum_{j\in\mathcal{J}} \frac{T}{\frac{F}{f_j}+\frac{1}{Bs_j}} \tag{20a}$$

$$\text{s.t.} \quad \text{Tr}(\boldsymbol{Z}_j\boldsymbol{V}_2) + |\eta_j|^2 \geq \frac{\sigma^2(2^{s_j}-1)}{p}, \forall j \in \mathcal{J} \tag{20b}$$

$$[\boldsymbol{V}_2]_{n,n} = 1, \forall n = 1,2,\cdots,N+1 \tag{20c}$$

$$\boldsymbol{V}_2 \succeq 0. \tag{20d}$$

To show the convexity of Problem (20), we define $q(s_j) = \frac{T}{A_j+\frac{1}{Bs_j}}$ and derive the second-order derivative of $q(s_j)$ as $\frac{\partial^2 q}{\partial s_j^2} = -\frac{2A_jB^2T}{(A_jBs_j+1)^3} < 0$. Thus, the objective function of maximizing $\sum_{j\in\mathcal{J}} q(s_j)$ is convex. We further note that the right hand side (RHS) of (20b) is convex with respect to s_j since $\frac{\partial^2 2^{s_j}}{\partial (s_j)^2} = 2^{s_j}(\ln 2)^2 \geq 0$, thus, constraint (20b) is convex as well. As such, we show that Problem (20) is convex.

With given $\boldsymbol{\Phi}_2$, the phase shift matrix for IRS 1 can be derived by

$$\max_{\boldsymbol{\Phi}_1,\boldsymbol{s}} \sum_{j\in\mathcal{J}} \frac{T}{\frac{F}{f_j}+\frac{1}{Bs_j}} \tag{21a}$$

$$\text{s.t.} \quad |\boldsymbol{W}_j^{\boldsymbol{H}}\boldsymbol{v} + \iota_j|^2 \geq \frac{\sigma^2(2^{s_j}-1)}{p}, \forall j \in \mathcal{J} \tag{21b}$$

$$|v_n|^2 = 1, \forall n \in \mathcal{N}, \tag{21c}$$

where $\boldsymbol{W}_j^{\boldsymbol{H}} = \boldsymbol{g}_{2,j}^{\boldsymbol{H}}[\text{diag}(\boldsymbol{u}_{1,1})\boldsymbol{r}, \cdots, \text{diag}(\boldsymbol{u}_{1,N})\boldsymbol{r}] + \boldsymbol{\Psi}_{1,j}$, $\iota_j = \boldsymbol{\Psi}_{2,j}\boldsymbol{r} + h_j^d$. We then follow similar procedures from (17) to (20) and reformulate the subproblem of phase shift matrix for IRS 1 as

$$\max_{\boldsymbol{V}_1,\boldsymbol{s}} \sum_{j\in\mathcal{J}} \frac{T}{\frac{F}{f_j}+\frac{1}{Bs_j}} \tag{22a}$$

$$\text{s.t.} \quad \text{Tr}(\boldsymbol{Q}_j\boldsymbol{V}_1) + |\iota_j|^2 \geq \frac{\sigma^2(2^{s_j}-1)}{p}, \forall j \in \mathcal{J} \tag{22b}$$

$$[\boldsymbol{V}_1]_{n,n} = 1, \forall n = 1,2,\cdots,N+1 \tag{22c}$$

$$\boldsymbol{V}_1 \succeq 0, \tag{22d}$$

where $\boldsymbol{V}_1 = \bar{\boldsymbol{v}}\bar{\boldsymbol{v}}^{\boldsymbol{H}}$ and

$$\boldsymbol{Q}_j = \begin{bmatrix} \boldsymbol{W}_j\boldsymbol{W}_j^{\boldsymbol{H}} & \iota_j\boldsymbol{W}_j \\ \iota_j^{\boldsymbol{H}}\boldsymbol{W}_j^{\boldsymbol{H}} & 0 \end{bmatrix}, \bar{\boldsymbol{v}} = \begin{bmatrix} \boldsymbol{v} \\ 1 \end{bmatrix}. \tag{23}$$

We observe that Problems (20) and (22) are semi-definite programming problems, and each of which can be solved efficiently by applying the SDR method with a complexity of $\mathcal{O}(\max(J,N)^4N^{1/2}\log_2(1/\epsilon))$ [13]. Note that the derived $\boldsymbol{V}_2$ and $\boldsymbol{V}_1$ cannot be guaranteed to satisfy the rank-one constraint. To tackle this issue, we adopt a similar randomization process as in [5] to obtain the near-optimal rank-one solutions of $\boldsymbol{V}_2$ and $\boldsymbol{V}_1$, which is omitted here for brevity.

D. Proposed Algorithm

We summarize our proposed solution in Algorithm 1 where the source node's transmit power, computing frequency allocation and phase shift matrices for double IRSs are optimized alternately.

Algorithm 1 Proposed Solution for Problem (7).

1: initialize: Set $(p^t, f_0^t, f_j^t, \boldsymbol{\Phi}_2^t, \boldsymbol{\Phi}_1^t)$ and $t = 1$.
2: **repeat**
3: Given $\{f_j^t, \boldsymbol{\Phi}_2^t, \boldsymbol{\Phi}_1^t\}$, obtain the optimal transmit power p^{t+1} and computing frequency f_0^{t+1} at the source node based on (10) and (11) respectively;
4: Given $\{p^{t+1}, f_0^{t+1}, \boldsymbol{\Phi}_2^t, \boldsymbol{\Phi}_1^t\}$, obtain the optimal computing frequency allocation for UEs f_j^{t+1} based on (15) and (16);
5: Given $\{p^{t+1}, f_0^{t+1}, f_j^{t+1}, \boldsymbol{\Phi}_1^t\}$, obtain the suboptimal phase shift matrix for IRS 2 $\boldsymbol{\Phi}_2^{t+1}$ based on (20);
6: Given $\{p^{t+1}, f_0^{t+1}, f_j^{t+1}, \boldsymbol{\Phi}_2^{t+1}\}$, obtain the suboptimal phase shift matrix for IRS 1 $\boldsymbol{\Phi}_1^{t+1}$ based on (22);
7: Update the iterative number $t = t + 1$;
8: **until** convergence.

Denote $D_{tot}(p^t, f_0^t, f_j^t, \boldsymbol{\Phi}_2^t, \boldsymbol{\Phi}_1^t)$ as the objective value in the t-th iteration, we have

$$\begin{aligned} D_{tot}(p^t, f_0^t, f_j^t, \boldsymbol{\Phi}_2^t, \boldsymbol{\Phi}_1^t) &\overset{(a)}{\leq} D_{tot}(p^{t+1}, f_0^{t+1}, f_j^t, \boldsymbol{\Phi}_2^t, \boldsymbol{\Phi}_1^t) \overset{(b)}{\leq} \\ D_{tot}(p^{t+1}, f_0^{t+1}, f_j^{t+1}, \boldsymbol{\Phi}_2^t, \boldsymbol{\Phi}_1^t) &\overset{(c)}{\leq} D_{tot}(p^{t+1}, f_0^{t+1}, f_j^{t+1}, \boldsymbol{\Phi}_2^{t+1}, \boldsymbol{\Phi}_1^t) \\ &\overset{(d)}{\leq} D_{tot}(p^{t+1}, f_0^{t+1}, f_j^{t+1}, \boldsymbol{\Phi}_2^{t+1}, \boldsymbol{\Phi}_1^{t+1}), \end{aligned} \tag{24}$$

where (a)-(d) hold due to the update of (p, f_0), f_j, $\boldsymbol{\Phi}_2$ and $\boldsymbol{\Phi}_1$ in Steps 3, 4, 5, and 6 of Algorithm 1, respectively. Thus, our proposed Algorithm 1 is guaranteed to converge. Since the complexity of Algorithm 1 is the addition of that in each step, thus, the overall complexity of Algorithm 1 is $O(2\log_2(1/\epsilon)+2(\max(J,N)^4N^{1/2}\log_2(1/\epsilon)))$, which shows that Algorithm 1 can be implemented within polynomial time in the worst scenario.

IV. Simulation Results

In this section, numerical results are provided to verify the interesting power allocation tradeoff in double IRSs and demonstrate the effectiveness of our proposed algorithm for enhancing the computing performance. We consider the source node is fixed at $(0\text{ m}, 0\text{ m})$ and $J = 6$ UEs are randomly distributed on a circle centered at $(100\text{ m}, 0\text{ m})$ with radius of 10 m. IRS 1 and IRS 2 each with $N = 16$ reflecting elements are deployed at $(45\text{ m}, 10\text{ m})$ and $(65\text{ m}, 10\text{ m})$, respectively. The channels of $\boldsymbol{h}_k, h_j^d$, $\boldsymbol{g}_{k,j}$ and $\boldsymbol{U}$ are generated based on the independent Rician distributions with a Rician factor of 5. We model the large-scale path loss as $-30-10\alpha\log_{10}(d)$ dB, where d is the corresponding distances and α is the path loss exponent. We set the path loss exponents for $\boldsymbol{h}_k, h_j^d$, $\boldsymbol{g}_{k,j}$ and $\boldsymbol{U}$ as $\alpha_k = 2.2, \alpha_j^d = 3$, $\alpha_{k,j} = 2.2$ and $\alpha_{IRS1,IRS2} = 2.2$, respectively. We set $F = 1000$ cycles/bit and $T = 200$ ms. The transmission bandwidth and noise power are set as $B = 0.1$ MHz and $\sigma^2 = -90$ dBm, respectively. We set $p_0^{max} = 2$ W and $p_{tot} = 6$ W, respectively.

Fig. 2 plots the relation between D_{tot} and source node's total transmit power $p_t = Jp$ with optimized $\{f_j, \boldsymbol{\Phi}_2, \boldsymbol{\Phi}_1\}$. We observe from Fig. 2 that there exists a unique optimal transmit power that maximizes D_{tot}, which verifies the tradeoff on power allocation for computing and transmitting at the source node. Moreover, we observe that when p_0^{max} increases from 2 to 4 W, the maximum D_{tot} follows a similar trend and increases from 0.678 to 0.773 MB. This is because with a

This article has been accepted for publication in a future issue of this journal, but has not been fully edited. Content may change prior to final publication. Citation information: DOI10.1109/lwc.2023.3243031, IEEE Wireless Communications Letters

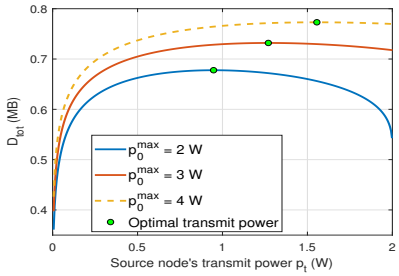

Fig. 2. D_{tot} versus source node's total transmit power p_t.

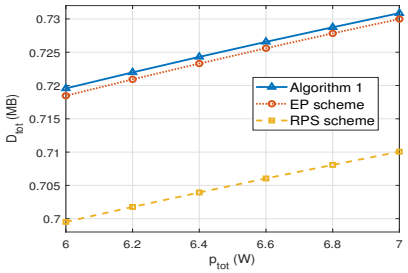

Fig. 3. Scheme comparison over a wide range of p_{tot}.

higher p_0^{max}, a larger D_{tot} is expected since more power can be used at the source node for local computing and transmission.

In Fig. 3, we compare the mean D_{tot} achieved by our proposed Algorithm 1 and the following two benchmark strategies based on 50 trials of randomization for all channels. 1) "Equal power allocation (EP)" scheme: in this scheme, the source node splits its power for computing and transmitting equally, i.e., $Jp = \kappa f_0^3 = p_0^{max}/2$, and each UE equally shares p_{tot}, i.e. $f_j = \sqrt[3]{\frac{p_{tot}}{J\kappa}}$. The phase shift matrices for double IRSs are solved based on (20) and (22), respectively; 2) "Random phase shift (RPS)" scheme: We set $\theta_{k,n} = 1, \forall k \in \{1, 2\}, \forall n \in \mathcal{N}$ and optimize all other variables with Algorithm 1. We observe that our proposed solution achieves the largest D_{tot} compared to the "EP" and "RPS" schemes over a wide range of p_{tot}, which emphasizes the importance of joint optimizing all variables. Specifically, when $p_{tot} = 6$ W, our proposed solution results in an average D_{tot} of 0.720 MB, while that of "EP" and "RPS " schemes are with 0.718 MB and 0.699 MB, respectively.

To show the superiority of double-IRS over single-IRS on maximizing D_{tot}, Fig. 4 is plotted with different numbers of reflecting elements N on each IRS based on 50 trials of randomization for all channels. In "Single-IRS" scheme, we consider the IRS 1 is with $2N$ reflecting elements and $\mathbf{\Phi}_2 = \mathbf{0} \in \mathbb{C}^{N \times N}$, and all other variables are optimized using Algorithm 1. It can be seen from Fig. 4 that the "Double-IRS" scheme outperforms the "Single-IRS" scheme. This is because in double-IRS solution, not only the single-reflection links and direct link, but also the double-reflection link is superimposed at each UE, resulting in a higher transmission rate and a larger D_{tot}. Moreover, we observe that with an increase of N, a larger D_{tot} can be achieved. This phenomenon can be explained since the more reflecting elements are deployed on each IRS, the higher the double-IRS beamforming gain can

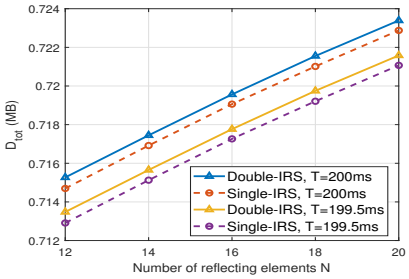

Fig. 4. D_{tot} versus different numbers of reflecting elements N on each IRS.

be achieved, which further leads to a larger D_{tot}. Moreover, we notice that a larger amount of tasks can be offloaded and computed within a longer time duration T.

V. Conclusions

We investigated the computing performance of double-IRS-aided cooperative computing systems and developed an efficient algorithm to maximize the total amount of computing task subject to latency and power constraints. Simulation results verified the power allocation tradeoff and validated the benefits of double IRSs in terms of improving the computing performance over benchmark strategies.

References

[1] Y. Zhou, C. Pan, P. L. Yeoh, K. Wang, M. Elkashlan, B. Vucetic, and Y. Li, "Secure Communications for UAV-Enabled Mobile Edge Computing Systems," in *IEEE Trans. Commun.,* vol. 68, no. 1, pp. 376-388, Jan. 2020.

[2] Y. Zhou, C. Pan, P. L. Yeoh, K. Wang, M. Elkashlan, B. Vucetic, and Y. Li, "Communication-and-Computing Latency Minimization for UAV-Enabled Virtual Reality Delivery Systems," in *IEEE Trans. Commun.,* vol. 69, no. 3, pp. 1723-1735, March 2021.

[3] Y. Zhang, B. Di, P. Wang, J. Lin, and L. Song, "HetMEC: Heterogeneous Multi-Layer Mobile Edge Computing in the 6G Era," in *IEEE Trans. Veh. Technol.* vol. 69, no. 4, pp. 4388-4400, April 2020.

[4] Y. Pan, C. Pan, K. Wang, H. Zhu, and J. Wang, "Cost Minimization for Cooperative Computation Framework in MEC Networks," in *IEEE Trans. Wireless Commun.,* vol. 20, no. 6, pp. 3670-3684, June 2021.

[5] Z. Ma, Y. Wu, M. Xiao, G. Liu, and Z. Zhang, "Interference Suppression for Railway Wireless Communication Systems: A Reconfigurable Intelligent Surface Approach," in *IEEE Trans. Veh. Technol.* vol. 70, no. 11, pp. 11593-11603, Nov. 2021.

[6] G. Zhou, C. Pan, H. Ren, K. Wang, M. D. Renzo, and A. Nallanathan, "Robust Beamforming Design for Intelligent Reflecting Surface Aided MISO Communication Systems," in *IEEE Wireless Commun. Lett.,* vol. 9, no. 10, pp. 1658-1662, Oct. 2020.

[7] Y. Zhou et al., "Latency Minimization for Secure Intelligent Reflecting Surface Enhanced Virtual Reality Delivery Systems," accepted in *IEEE Wireless Commun. Lett.,* 2022.

[8] Y. Zhang, B. Di, H. Zhang, Z. Han, H. Vincent Poor, and L. Song, "Meta-Wall: Intelligent Omni-Surfaces Aided Multi-Cell MIMO Communications," accepted in *IEEE Trans. Wireless Commun.,* 2022.

[9] T. Bai, C. Pan, Y. Deng, M. Elkashlan, A. Nallanathan, and L. Hanzo, "Latency Minimization for Intelligent Reflecting Surface Aided Mobile Edge Computing," in *IEEE J. Sel. Areas Commun.,* vol. 38, no. 11, pp. 2666-2682, Nov. 2020.

[10] S. Mao, X. Chu, Q. Wu, L. Liu, and J. Feng, "Intelligent Reflecting Surface Enhanced D2D Cooperative Computing," in *IEEE Wireless Commun. Lett.,* vol. 10, no. 7, pp. 1419-1423, July 2021.

[11] B. Zheng, C. You, and R. Zhang, "Double-IRS Assisted Multi-User MIMO: Cooperative Passive Beamforming Design," in *IEEE Trans. Wireless Commun.,* vol. 20, no. 7, pp. 4513-4526, July 2021.

[12] B. Zheng, C. You and R. Zhang, "Efficient Channel Estimation for Double-IRS Aided Multi-User MIMO System," in *IEEE Trans. Commun.,* vol. 69, no. 6, pp. 3818-3832, June 2021.

[13] Z.-Q. Luo, W.-K. Ma, A.M.-C. So, Y. Ye, and S. Zhang, "Semidefinite Relaxation of Quadratic Optimization Problems," in IEEE Signal Process. Mag., vol. 27, no. 3, pp. 20-34, May 2010.